Calculated Potential Energy Curves of OH

IAN EASSON AND M. H. L. PRYCE
Department of Physics, University of British Columbia, Vancouver 8, British Columbia
Received August 24, 1972[1]

A configuration-interaction calculation of the electronic energies of the OH radical has been performed, using from 34 to 46 configurations for the doublet states; and from 11 to 25 configurations for the quartet states. The results are presented for the six lowest states of $^2\Sigma^+$, $^2\Sigma^-$, $^2\Pi$, $^2\Delta$; $^4\Sigma^+$, $^4\Sigma^-$, $^4\Pi$, and $^4\Delta$ symmetries. The calculations have been performed for a range of internuclear distances from 0.8 to 3 Å. The method of computation has been designed to give the kind of accuracy for the lowest three or four states of each symmetry which could be useful in the empirical analysis of the hitherto unanalyzed spectrum of OH in the 1850 Å region.

Nous avons calculé l'énergie électronique de plusieurs niveaux de l'OH, utilisant de 34 à 46 configurations pour les niveaux doublets, et de 11 à 25 configurations pour les niveaux quartets, tenant compte de l'interaction de configuration. Nous présentons les résultats pour les six niveaux inférieurs de symmétrie $^2\Sigma^+$, $^2\Sigma^-$, $^2\Pi$, $^2\Delta$; $^4\Sigma^+$, $^4\Sigma^-$, $^4\Pi$ et $^4\Delta$. Les calculs furent éxécutés pour des distances internucléaires de 0.8 à 3 Å. Le calcul fut effectué d'une telle manière que la précision soit suffisante à tenter l'analyse empirique du spectre jusqu'ici inanalysé de l'OH dans la région de 1850 Å.

Can. J. Phys., **51**, 518 (1973)

Introduction

There are five known bound electronic states of the hydroxyl radical OH. The ground state, $X^2\Pi$, and three excited states, A, B, and $C^2\Sigma^+$, have been known for some time (Herzberg 1950). Recently, a bound $^2\Sigma^-$ state was found[2], which in the present work is referred to as the $D^2\Sigma^-$ state. A knowledge of the potential energy curves of some of the other electronic states of OH would be useful for the following two reasons.

Michel (1957) observed a series of emission lines with a complicated structure in the 1850 Å region. These lines have been tentatively interpreted (Felenbok 1963) as due to transitions from the low vibrational levels of the $C^2\Sigma^+$ state to the high vibrational levels of the $X^2\Pi$ state. Other interpretations may be possible, and even likely. It would be valuable to have additional potential energy curves of OH in order to suggest other interpretations.

The hydroxyl radical has been detected in galactic clouds. For a review, see Terzian and Scharlemann (1970). It appears that the OH is forming a natural maser. Several mechanisms for producing population inversion in these clouds have been proposed. More knowledge about the as yet undetected electronic states of OH may help to elucidate possible pumping mechanisms.

For these reasons, a calculation from first principles of some of the lower-lying potential energy curves of OH would be of value. Such a calculation has been performed, and some of the results are reported here. To the best of the authors' knowledge, the only potential energy curves of OH which have been calculated so far are those of the $X^2\Pi$ state (Cade and Huo 1967; Michels and Harris 1969) and the lowest $^2\Sigma^-$, $^2\Sigma^+$, $^4\Sigma^-$, and $^4\Pi$ states (Michels and Harris 1969).

The method of calculation used is outlined in Part I of this paper. In Part II, calculated potential energy curves of the lowest few $^2\Sigma^-$, $^2\Sigma^+$, $^2\Pi$, $^2\Delta$, $^4\Sigma^-$, $^4\Sigma^+$, $^4\Pi$, and $^4\Delta$ electronic states are given. Qualitative information is presented about some of the wave functions. Comparisons are made with experimental data and with other OH calculations.

Part I: Method of Calculation

It is not necessary to calculate highly accurately a very large number of potential energy curves in order to aid in solving problems such as those mentioned in the Introduction. The calculation of the lowest few curves of each symmetry type will probably suffice for a first approach such as this work. Furthermore, for present purposes relative energies are more important than ab-

[1]Revision received November 27, 1972.
[2]Douglas, A. E. "Absorption of OH in the 1200 Å region". To be published.

solute energies. Finally, the shape of each curve needs only to be calculated accurately enough to predict approximately the depth of its potential energy minimum and the corresponding equilibrium distance. These considerations were kept in mind in formulating the following method of calculation. It was designed to produce relative energies for the lowest few (three or four) states of each symmetry type to the accuracy just mentioned.

The wave functions were linear superpositions of configurations. At a given internuclear distance, and for a given symmetry type, the linear coefficients in the wave function were determined in the usual manner by calculating and diagonalizing the Hamiltonian matrix. The use of many configurations allowed several states of one symmetry type to be calculated together and permitted a state to change configurations with changing internuclear distance. Each configuration was a linear combination of Slater determinants. The molecular orbitals forming the Slater determinants were constructed by Schmidt orthogonalization of a set of atomic orbitals.

The atomic orbitals used were $1s$, $2s$, $2p\tilde{\pi}$, $2p\sigma$, $2p\pi$, $3s$, $3p\tilde{\pi}$, $3p\sigma$, $3p\pi$, $3d\tilde{\delta}$, $3d\tilde{\pi}$, $3d\sigma$, $3d\pi$, and $3d\delta$ centered on oxygen and $1s$, $2s$, $2p\tilde{\pi}$, $2p\sigma$, and $2p\pi$ centered on hydrogen. It will be convenient in the discussion that follows to divide the atomic orbitals into two classes: atomic orbitals of the first kind, which occur in the ground states of O and H, and atomic orbitals of the second kind, which occur only in excited states of O and H. For notational convenience, an atomic orbital whose center is not given is assumed to be centered on oxygen. For example, $1s$ means $(1s)_O$.

Each atomic orbital was represented by a single Slater-type orbital. A Slater-type orbital has a radial dependence of the form $r^{n-1}e^{-\xi r}$, where n is the principal quantum number, and ξ is an orbital parameter. Because of computer limitations, it was not possible to use a linear combination of two or more Slater-type orbitals per atomic orbital without unduly reducing the number of configurations. It may be objected that the use of only one Slater-type orbital per atomic orbital can sometimes lead to large inaccuracies. This possible criticism will be answered later in this section.

The nine σ molecular orbitals were constructed by orthogonalizing in the order $(1s, 2s, 2p\sigma)_O$, $(1s)_H$, $(3s, 3p\sigma, 3d\sigma)_O$, $(2s, 2p\sigma)_H$. The four π molecular orbitals were formed similarly from $(2p\pi, 3p\pi, 3d\pi)_O$, $(2p\pi)_H$. One δ molecular orbital was used, consisting of a single $(3d\delta)_O$ atomic orbital.

Each molecular orbital had one atomic orbital which was its main constituent. Two kinds of molecular orbitals can then be defined, corresponding to the two kinds of atomic orbitals. It is here supposed that molecular orbitals of the second kind are most important in the excited state wave functions of OH. In what follows, a molecular orbital is denoted by the atomic orbital which is its main constituent. For example, the $(1s)_H$ molecular orbital is the one which is mainly $(1s)_H$, with admixtures of the $1s$, $2s$, and $2p\sigma$ atomic orbitals.

It is well known that there is another way to divide molecular orbitals into two classes, depending on an orbital's behavior as the internuclear distance is changed adiabatically. Valence electron orbitals change significantly, whereas core orbitals change relatively little. Similarly, at a fixed internuclear distance, the lowest few electronic states differ mainly in their valence electron wave functions, whereas corresponding core orbitals in the different states are very similar.

If the shapes of the lowest few potential energy curves and their relative spacings are the only points of interest, as is the case here, then two things are suggested by the different behavior of core and valence orbitals. The first is that the valence electron parts of the wave functions should be treated accurately because of their great sensitivity. The second is that it is not necessary to treat the core orbitals as accurately as the valence orbitals, because the error in energy arising from an approximate core wave function should be quite insensitive to internuclear distance or electronic state.

These considerations are the basis of a method of potential energy curve calculation due to Das and Wahl (1967) and which has had good success. There, an approximate core wave function of Hartree–Fock accuracy is used in conjunction with a valence electron wave function which is a superposition of different valence configurations. The form of wave function used here is similar to that used by Das and Wahl (1967), with modifications as noted below.

The core wave function used was $(1s)^2(2s)^2$. The identification of this as the core is based on two considerations. First, the orbital parameters

ξ_{1s} and ξ_{2s} depend only very weakly on internuclear distance (Easson 1971), whereas the other ξ_i vary strongly with changing internuclear distance. Secondly, it was found after extensive preliminary calculations that configurations in which the $1s$ or $2s$ molecular orbital is only singly occupied contributed very little to the wave functions of the lower energy states. An important exception occurred for states of $^2\Sigma^+$ symmetry. It was found that some $^2\Sigma^+$ configurations in which one electron was promoted from a $2s$ to a $2p\sigma$ orbital were rather low lying in energy. These configurations were retained in the final calculation.

Because only one Slater-type orbital was used per atomic orbital, the $(1s)^2(2s)^2$ core was of slightly less than Hartree–Fock accuracy. For a more quantitative discussion of this point, see Part II*a*. However, the same arguments which can be employed to justify the use of only a Hartree–Fock core can also be used to justify a core of slightly less than Hartree–Fock accuracy. It seems likely then that the calculated relative energies would not be significantly changed if more than one Slater-type orbital were used for each of the $1s$ and $2s$ atomic orbitals.

The choice of configurations is now discussed. Apart from the exception noted previously, and a few others, all configurations contained a $(1s)^2(2s)^2$ core. The remaining 5 electrons can be distributed amongst the 17 valence orbitals in a large number of ways, and it was not possible in practise to retain all these valence configurations. For the spin doublet calculations, the average number of configurations chosen per symmetry type was 40; for the quartets, 21. It ranged from 34 to 46, and from 11 to 25 respectively.

In selecting configurations, the division of orbitals into those of the first and those of the second kind is very helpful. All valence configurations consisting entirely of valence orbitals of the first kind should be, and were, included. It is highly desirable that all configurations involving one valence orbital of the second kind be included, since it is these orbitals that can be expected to play an important role in excited states. All such configurations were included, with the following exception. In the Π calculations, a small number of configurations which contain one molecular orbital of the second kind could not be included for reasons of computer memory space. The consequences of these omissions are discussed in Part II*a*.

There are a very large number of possible configurations with more than one molecular orbital of the second kind. These configurations are generally higher in energy than those with at most one molecular orbital of the second kind, and each can be expected to have only a small effect on the lower energy states. Such configurations were not included.

The preceding contentions about the relative unimportance of these configurations to the lowest few states were verified by a number of preliminary calculations in which several of these configurations were included. The effect of these extra configurations on the states of interest was quite small. The stability of the present calculations with respect to the addition of extra configurations also suggests that the use of more than one Slater-type orbital per valence atomic orbital would not change the results significantly.

One consequence of the omission of these extra configurations, however, is the neglect of the dispersion energy connected with van der Waals' forces, since it is precisely these kinds of configurations which in the London theory of dispersion forces give rise to dispersion. This means that the present calculations are unable to reproduce correctly the shallow minima at large internuclear separations which are characteristic of the van der Waals' interaction.

Consider a calculation at a fixed internuclear distance, using a basis set of N configurations of the same symmetry type. Let ε_i, $i = 1, \ldots, N$ be the calculated eigenvalues. The ε_i depend on the orbital parameters ξ_i appearing in the exponentials of the Slater-type orbitals. The question arises as to what are the 'best' values of the orbital parameters to use.

The answer to this question depends on the state or states of interest. If only the lowest root is of concern to the calculator, the ξ_i's should be varied until ε_1 is a minimum. The set of ξ_i's for ε_1 is denoted $\xi_i^{(1)}$. This procedure will produce a good lowest state wave function, but the higher state wave functions will in general be poor, because the parameter values $\xi_i^{(1)}$ do not provide good excited orbitals. Most calculations to date use this approach, but it is not useful here, because more than just the lowest root is of interest.

If the second root is also of interest, ε_2 should be minimized by varying a new set of parameters

$\xi_i^{(2)}$. However, the trial wave function for the second root must be constrained to be orthogonal to the previously found optimized wave function for the lowest root. A similar procedure can be followed for the higher roots.

The constraint that a trial wave function be orthogonal to the optimized wave functions of the lower roots can be exceedingly important. This contention was verified by preliminary calculations in which ε_2 was subjected to unconstrained minimizations, with poor results. As ε_2 decreased, ε_1 increased. Although diagonalization guaranteed that the second state trial wave function was orthogonal to the wave function corresponding to the lowest root, the latter wave function differed more and more from the optimized first state wave function as ε_2 decreased. These preliminary calculations also showed that $\varepsilon_2, \varepsilon_3 \ldots$ were usually more sensitive to changes in the parameters of atomic orbitals of the second kind than was ε_1. The reason for this behavior is that atomic orbitals of the second kind are mainly important in excited states.

The successive minimization of $\varepsilon_1, \varepsilon_2, \ldots$ described above suffers from one great practical drawback. It requires as many sets of parameters $\xi_i^{(1)}, \xi_i^{(2)}, \ldots$ as there are states of interest. Practical considerations in the present case demanded the use of only one orbital parameter set ξ_i. This, coupled with the interest in more than one state, rendered the strict use of the variational principle inapplicable and made it necessary to devise a heuristic procedure to determine the single set of parameters ξ_i. Any procedure whatsoever designed to find the 'best' ξ_i in this case may be criticized as being somewhat arbitrary, since the variational procedure can no longer provide an unambiguous definition of what 'best' means.

The heuristic procedure adopted in this work is based on points which were brought out in the preceding discussion of the variational approach. The first point is the importance of the orthogonality constraint, and the second is the relevance to this problem of the distinction between atomic orbitals of the first and second kind.

It is of overriding importance to have a good approximation to the wave function of the lowest energy state, because the better the approximation the more nearly are the trial wave functions for all other states orthogonal to the exact wave function of that state. For this reason the orbital parameters for atomic orbitals of the first kind were determined by minimizing ε_1, because these orbitals are extremely important to the state of lowest energy.

In order to determine the parameters for atomic orbitals of the second kind we have seen that higher states than the first should somehow be taken into account. One way to do this, and the way chosen here, is by a pseudo-variational procedure, wherein a function of $\varepsilon_1, \varepsilon_2, \ldots$ is minimized with respect to variations in these parameters. This function has been chosen to reflect the primary importance of the lowest state, the secondary importance of the second lowest state, and so on, an order of importance which is suggested by the orthogonality constraints. Accordingly, the function was chosen to be a weighted sum of the ε_i, with most weight given to ε_1, less weight to ε_2, and so on. The actual weights used were $2^{-(i-1)}$ for $i = 1, \ldots, 5$, and 0 for $5 < i < N$.

It is very time-consuming to determine the orbital parameters by this method at all chosen internuclear distances. Instead, the parameters were determined this way at only 0.8, 1.0, 1.4, and 3.0 Å. At other distances, they were determined by piecewise polynomial interpolation from their values at the selected distances. Even so, to determine a new set of parameters for each different symmetry type is still time-consuming. The parameters for some symmetry types were taken from other similar symmetry types. For example, the $^4\Pi$ parameters were taken to be the same as the $^2\Pi$ parameters.

Further computational details can be found in Easson (1971), although the numerical results there have been superseded.

Part II: Results and Discussion

The potential energy curves for each of the lowest six states of $^2\Pi$, $^2\Sigma^+$, $^2\Sigma^-$, $^2\Delta$, $^4\Pi$, $^4\Sigma^+$, $^4\Sigma^-$, and $^4\Delta$ symmetry are given in Figs. 1 to 8 respectively. Figure 9 is a composite of Figs. 1 to 8. Figure 10 is a comparison of the calculated $X^2\Pi$ and $A^2\Sigma^+$ potential curves with curves determined from experimental data and with the curves for these states as calculated by other authors. Table 1 gives qualitative information about the wave functions of some of the states[3]. It lists the states of a particular symmetry

[3]The complete set of wave functions is available, at a nominal charge, from the Depository of Unpublished Data, National Science Library, National Research Council of Canada, Ottawa, Canada, K1A 0S2.

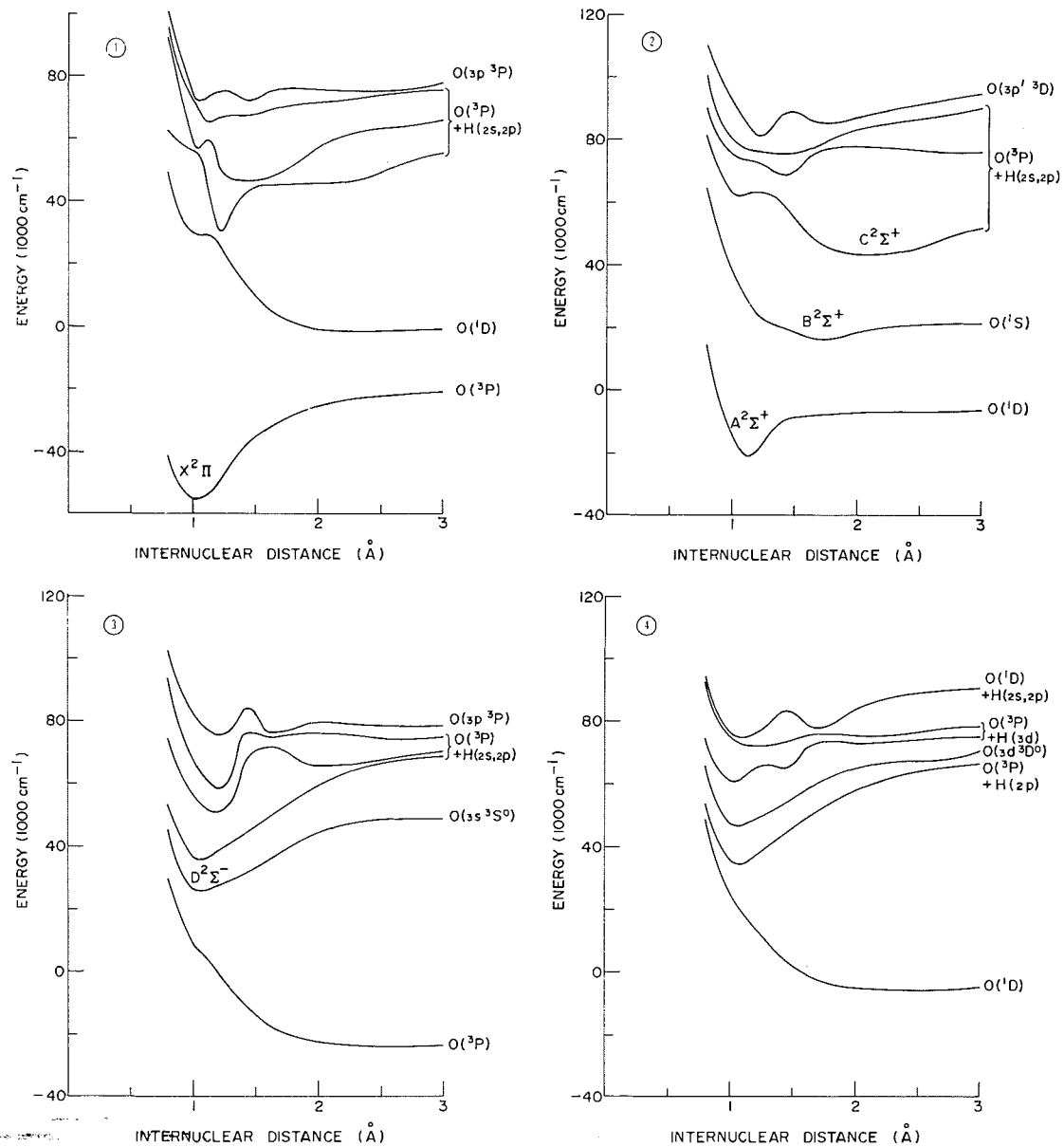

FIG. 1. Calculated $^2\Pi$ potential energy curves. In this and other figures, the states of O and H into which the molecular states should dissociate are listed on the right-hand side. The notation for the O states is that of Moore (1949). Unless otherwise given, the H state is H(1*s*). The zero of energy has been arbitrarily set at −75.0 hartrees.

FIGS. 2–4. Calculated $^2\Sigma^+$, $^2\Sigma^-$, and $^2\Delta$ potential energy curves respectively.

that are calculated to be bound, their calculated equilibrium separations, and the valence electron parts of the dominant configurations at equilibrium. The separations have been rounded off to the nearest 0.1 Å, because they are not more accurate than 0.1 Å for some of the higher excited states and also for the very slightly bound states with shallow potential wells.

Table 2 gives the calculated energies of all 48 states at 8 different internuclear separations. In Table 3 are listed the calculated and observed energy differences (ΔT_e) between the bottoms of

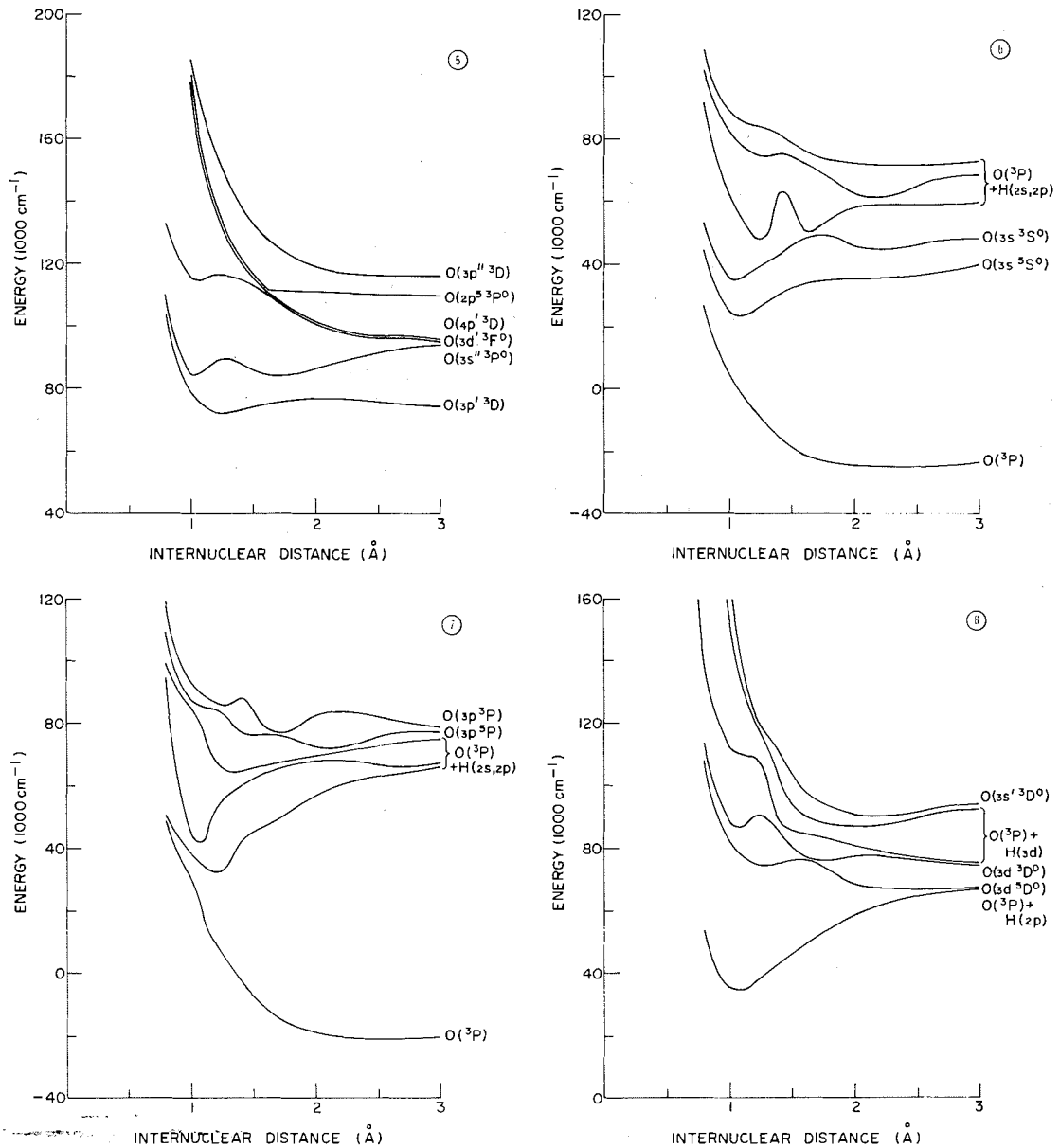

FIGS. 5–8. Calculated $^4\Sigma^+$, $^4\Sigma^-$, $^4\Pi$, and $^4\Delta$ potential energy curves respectively.

the potential wells of the $X^2\Pi$, $A^2\Sigma^+$, $B^2\Sigma^+$, $C^2\Sigma^+$, and $D^2\Sigma^-$ states.

(a) $^2\Pi$ *States*

Figure 1 gives the $^2\Pi$ curves. The lowest curve is that of the $X^2\Pi$ ground state. There is good agreement between the predicted and observed equilibrium separations (see Table 1). The dissociation energy calculated from Table 2 is about 0.85 of the observed value (Herzberg 1950).

The calculated $X^2\Pi$ curve will now be compared with two other published calculations of it and with an 'experimental' curve. The latter was computed by the methods of Klein (1932) and Rydberg (1931, 1933) from the spectroscopic data of Dieke and Crosswhite (1948) for $v = 0$,

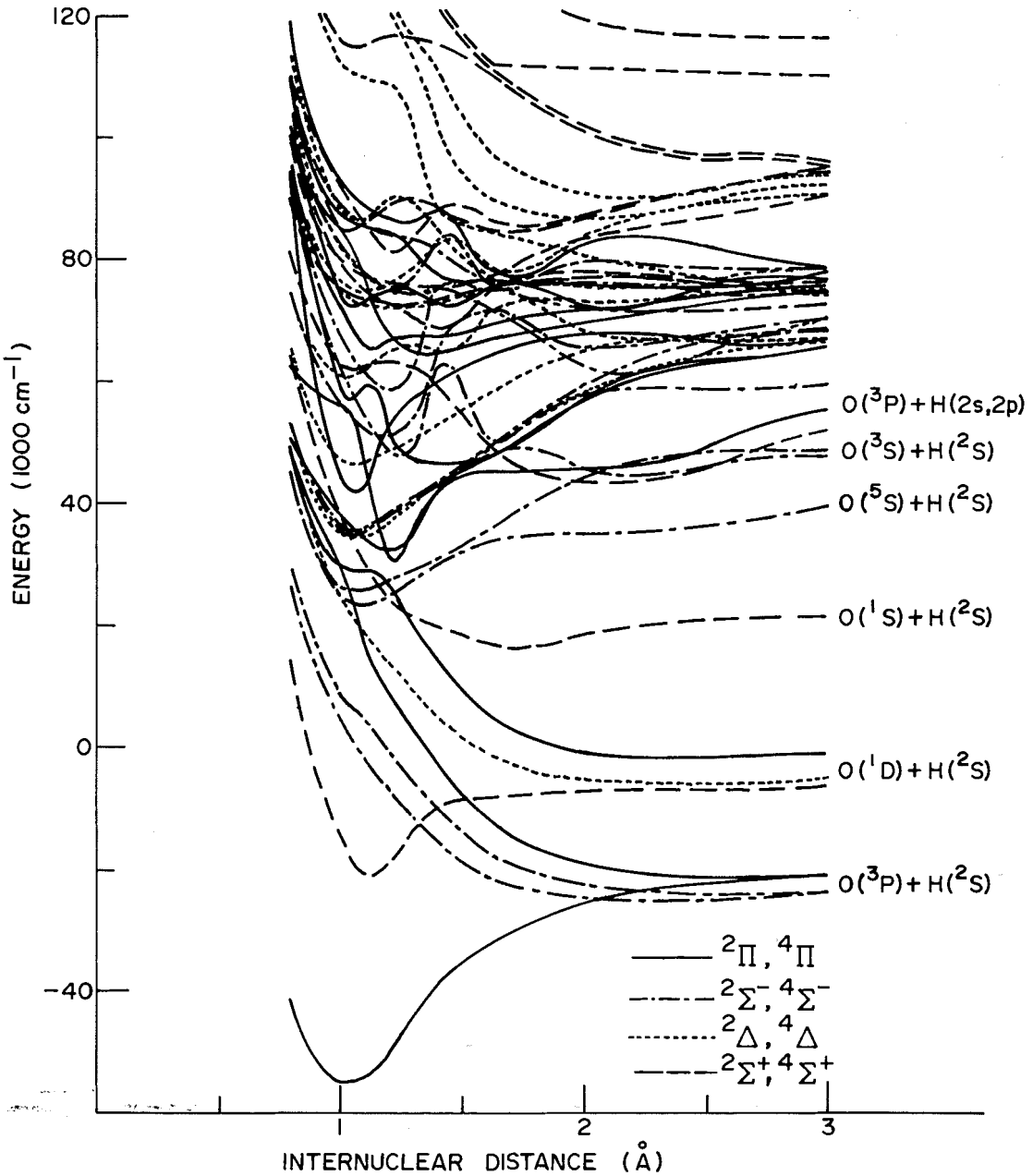

FIG. 9. This figure is a composite of Figs. 1 to 8. It shows all the calculated potential energy curves in relation to one another.

1, 2, and 3; of Herman and Hornbeck (1953) for $v = 4$, 5, and 6; of Chamberlain and Roesler (1955) for $v = 8$ and 9; of Cawthon and McKinley (1956) for $v = 4$, 5, 6, 7, 8, and 9; and from a tentative analysis of the OH spectrum in the 1850 Å region (Dalby and Douglas, unpublished) by one of us (MHLP) for $v = 12$, 13, and 14. It was fitted to the dissociation energy of Carlone and Dalby (1969).

Cade and Huo (1967) performed a Hartree–Fock calculation of the $X^2\Pi$ curve in the region of its minimum. This curve is given in Fig. 10, along with the 'experimental' curve, our curve, and the curve of Michels and Harris (1969),

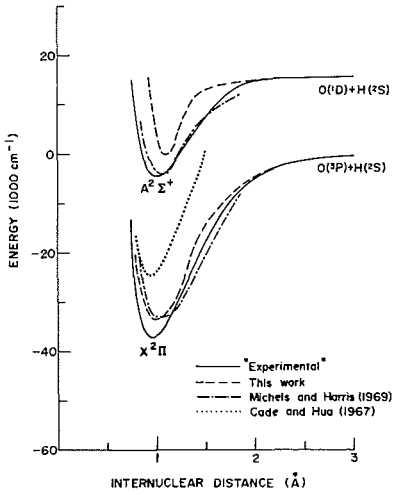

FIG. 10. Calculated and "experimental" potential energy curves for the $X^2\Pi$ and $A^2\Sigma^+$ states.

whose wave function was also a linear superposition of configurations. In Fig. 10, the zero of energy is taken to be the energy of the separated atoms $O(^3P) + H(^2S)$. Michels and Harris (1969) did not quote absolute energies. Their curve has therefore been shifted so as to dissociate to the zero of energy at large internuclear distances. For comparison purposes, our curve has been similarly shifted.

Since Cade and Huo (1967) did not carry their calculation to large internuclear distances, where Hartree–Fock calculations are often quite unreliable, their curve could not be shifted as the other two calculated curves have been. Rather, it has been placed so that the difference between their absolute minimum of energy and a Hartree–Fock calculation of the separated atom energy is faithfully reproduced.

The placement of our $X^2\Pi$ curve below the Hartree–Fock one in Fig. 10 should not obscure the fact that the absolute $X^2\Pi$ minimum energy in the present calculation, namely -75.25 hartrees, is 0.17 hartree above the Hartree–Fock value of -75.42 hartrees (Cade and Huo 1967). The reason for this situation is that our $(1s)^2(2s)^2$ core is of slightly less than Hartree–Fock accuracy, coupled with the fact that the energy of this core is by far the most important part of the total electronic energy (Cade and Huo 1967). An underestimate of the Hartree–Fock core energy by about 0.5% would lead to a total discrepancy of about 0.17 hartree. It must be emphasized that, for reasons stated in Part I, this comparison of the two absolute energies does not imply any similar error in the present predictions of relative energies.

Figure 10 shows that the Michels and Harris (1969) curve and ours are quite similar, with ours slightly better at small internuclear distances, and slightly worse at large internuclear distances. Both predict about the same dissociation energy and equilibrium internuclear distance.

The vibration frequency ω_e for $X^2\Pi$, as calculated from the data in Table 2, is about 3758 cm^{-1}. This value compares quite favorably with the experimental value of 3735.21 cm^{-1} (Herzberg 1950).

The first excited $^2\Pi$ state, which arises from $O(^1D)$ and $H(^2S)$, is predicted to be unbound. The discussion in Part I about the neglect of dispersion energy in the calculations should be noted in the case of this and all other states which are predicted to be unbound. Carlone and Dalby (1969) had suggested that if this state were bound, the predissociation which is observed to set in near vibrational quantum number $v = 4$ or 5 in the $A^2\Sigma^+$ state could be explained. The present calculations do not support this suggestion. For a more recent interpretation of this predissociation at high v, see Czarny *et al.* (1971).

As noted in Part I, a few configurations which it would be desirable to include in the $^2\Pi$ and $^4\Pi$ calculations could not be included because of computer constraints. As a result, the calculated $X^2\Pi$ and the lowest $^4\Pi$ curves do not dissociate to quite the same energy as the calculated $^2\Sigma^-$ and $^4\Sigma^-$ curves do, as they should since all four states arise from $O(^3P)$ and $H(^2S)$ (see Fig. 9). The discrepancy is about 4000 cm^{-1}. Similarly, the curve calculated for first excited $^2\Pi$ state does not dissociate to quite the same energy as the calculated curves for the lowest $^2\Sigma^+$ and $^2\Delta$ states. The inclusion of these configurations will bring the dissociated energies into agreement. There may be another effect of these omissions. The higher excited $^2\Pi$ and $^4\Pi$ curves, probably from the third excited states and up, may not be as reliable as the other curves.

(b) $^2\Sigma^+$ *States*

The $^2\Sigma^+$ curves are given in Fig. 2. The predicted equilibrium separations for the A, B, and $C^2\Sigma^+$ states are in good agreement with experiment (see Table 1). The corresponding dissocia-

TABLE 1. Calculated bound states of OH

Symmetry type	State number	Equilibrium distances (Å)[a]	Dominant valence electron configurations at equilibrium[b]
$^2\Sigma^+$	1[c]	1.1[d]	$(2p\sigma)(2p\pi)^2(2p\bar{\pi})^2$, $(1s)_H(2p\pi)^2(2p\bar{\pi})^2$
	2[e]	1.8[f]	$(2p\sigma)^2(2p\pi)(2p\bar{\pi})(1s)_H$
	3[g]	2.1[h]	$(2p\sigma)(2p\pi)^2(2p\bar{\pi})^2$
	4	1.4	$(2p\sigma)^2(2p\pi)(2p\bar{\pi})(3s)$
	5	1.3	$(2p\sigma)(2p\pi)^2(2p\bar{\pi})[^3\Pi](3d\bar{\pi})$, $(1s)_H(2p\pi)^2(2p\bar{\pi})^2$
	6	1.2	$(2p\sigma)^2(2p\pi)(2p\bar{\pi})(3p\sigma)$
	6	1.6	$(2p\sigma)(2p\pi)(2p\bar{\pi})^2(2p\pi)_H$
$^2\Sigma^-$	2[i]	1.0[j]	$(2p\sigma)^2(2p\pi)(2p\bar{\pi})(3p\sigma)$
	3	1.0	$(2p\sigma)^2(2p\pi)(2p\bar{\pi})(3d\sigma)$
	4	1.2	$(2p\sigma)^2(2p\pi)(2p\bar{\pi})(3d\sigma)$
	4	2.1	$(2p\pi)(2p\bar{\pi})[^3\Sigma](2p\sigma)(1s)_H^2$, $(2p\pi)(2p\bar{\pi})[^3\Sigma](2p\sigma)[^2\Sigma](3s)[^3\Sigma](1s)_H$
	5	1.3	$(2p\sigma)^2(2p\bar{\pi})^2(3d\delta)$
	6	1.2	$(2p\sigma)(2p\pi)^2(2p\bar{\pi})[^3\Pi](3d\bar{\pi})$
	6	1.6	$(2p\sigma)(2p\pi)^2(2p\bar{\pi})[^3\Pi](3d\bar{\pi})$
$^2\Pi$	1[k]	1.0[l]	$(2p\sigma)^2(2p\pi)^2(2p\bar{\pi})$
	3	1.2	$(2p\sigma)^2(2p\pi)(2p\bar{\pi})[^3\Sigma](3d\pi)$
	4	1.4	$(2p\sigma)^2(2p\pi)^2(2p\bar{\pi})$
	5	1.1	$(2p\sigma)^2(2p\pi)(2p\bar{\pi})[^3\Sigma](3p\pi)$, $(2p\sigma)^2(2p\pi)(2p\bar{\pi})[^3\Sigma](2p\pi)_H$
	6	1.1	$(2p\sigma)^2(2p\pi)(2p\bar{\pi})[^1\Sigma](3d\pi)$
	6	1.4	$(2p\sigma)^2(2p\pi)(2p\bar{\pi})[^3\Sigma](2p\pi)_H$
$^2\Delta$	2	1.1	$(2p\sigma)^2(2p\pi)(2p\bar{\pi})[^3\Sigma](3d\delta)$
	3	1.1	$(2p\sigma)^2(2p\pi)^2(3p\sigma)$, $(2p\sigma)^2(2p\pi)^2(3s)$
	4	1.0	$(2p\sigma)^2(2p\pi)^2(3d\sigma)$, $(2p\sigma)^2(2p\pi)^2(3p\sigma)$
	5	1.2	$(2p\sigma)(2p\pi)^2(2p\bar{\pi})[^3\Pi](3d\pi)$
	6	1.1	$(2p\sigma)(2p\pi)^2(2p\bar{\pi})[^3\Pi](3d\pi)$
	6	1.7	$(2p\sigma)(2p\pi)^2(1s)_H^2$, $(2p\sigma)(2p\pi)^2(3s)[^1\Delta](1s)_H$
$^4\Sigma^+$	1	1.2	$(2p\sigma)(2p\pi)(2p\bar{\pi})^2(3d\pi)$
	2	1.0	$(2p\sigma)(2p\pi)(2p\bar{\pi})^2(3p\pi)$
	2	1.7	$(2p\sigma)(2p\pi)(2p\bar{\pi})^2(2p\pi)_H$
$^4\Sigma^-$	2	1.1	$(2p\sigma)^2(2p\pi)(2p\bar{\pi})(3s)$, $(2p\sigma)^2(2p\pi)(2p\bar{\pi})(3p\sigma)$
	3	1.0	$(2p\sigma)^2(2p\pi)(2p\bar{\pi})(3d\sigma)$
	3	2.2	$(2p\sigma)(2p\pi)(2p\bar{\pi})[^4\Sigma](3s)[^3\Sigma](1s)_H$
	4	1.2	$(2p\sigma)^2(2p\pi)(2p\bar{\pi})(3d\sigma)$
	4	1.6	$(2p\sigma)(2p\pi)(2p\bar{\pi})[^4\Sigma](3s)[^3\Sigma](1s)_H$
	5	2.1	$(2p\sigma)(2p\pi)(2p\bar{\pi})[^4\Sigma](3d\sigma)[^3\Sigma](1s)_H$
$^4\Pi$	2	1.2	$(2p\sigma)^2(2p\pi)(2p\bar{\pi})(3d\pi)$
	3	1.1	$(2p\sigma)^2(2p\pi)(2p\bar{\pi})(3p\pi)$
	4	1.3	$(2p\sigma)(2p\pi)^2(2p\bar{\pi})(3s)$
	5	2.1	$(2p\sigma)(2p\pi)^2(2p\bar{\pi})(3s)$
	6	1.7	$(2p\sigma)(2p\pi)^2(2p\bar{\pi})(3d\sigma)$
$^4\Delta$	1	1.0	$(2p\sigma)^2(2p\pi)(2p\bar{\pi})(3d\delta)$
	5	2.0	$(2p\sigma)(2p\pi)^2(2p\bar{\pi})(3d\pi)$, $(2p\sigma)(2p\pi)^2(2p\bar{\pi})(2p\pi)_H$
	6	2.1	$(2p\sigma)^2(2p\pi)(2p\bar{\pi})(3d\delta)$, $(2p\pi)(2p\bar{\pi})[^1\Sigma](2p\sigma)(3d\delta)(1s)_H$

[a]Rounded off to nearest 0.1 Å.
[b]Spin coupling given in square brackets.
[c]$A^2\Sigma^+$ state.
[d]Experiment gives 1.01 Å (Carlone and Dalby 1969).
[e]$B^2\Sigma^+$ state.
[f]Experiment gives 1.79 Å (Carlone and Dalby 1969).
[g]$C^2\Sigma^+$ state.
[h]Experiment gives 2.05 Å (Carlone and Dalby 1969).
[i]$D^2\Sigma^-$ state.
[j]Experiment gives 1.07 Å.[2]
[k]$X^2\Pi$ state.
[l]Experiment gives 0.97 Å (Herzberg 1950).

tion energies, as estimated from the data in Table 2, are in fair accord with observation (Carlone and Dalby 1969). For the $A^2\Sigma^+$ state, the calculated dissociation energy is about 0.7 of the actual energy. The B state potential well is calculated to be about twice as deep as the actual extremely shallow well. The calculated curve for the C state is still rising sharply at 3 Å, the largest internuclear distance at which calculations were performed, but one knows that it dissociates to $O(^3P) + H(2p)$. One can therefore estimate the "calculated" dissociation energy at

TABLE 2. Calculated energies of states of OH at various internuclear distances.[a] Zero of energy is −75.0 hartrees

State	Internuclear distance (Å)							
	0.8	1.0	1.2	1.4	1.6	2.0	2.6	3.0
$^2\Sigma^+$	14.41[b]	−14.62	−19.42	−9.96	−8.14	−7.08	−6.63	−6.04
	64.48[c]	38.08	24.06	20.16	17.18	18.85	20.98	21.88
	81.49[d]	63.25	64.51	59.95	50.18	43.64	47.54	52.09
	90.13	75.37	72.69	69.25	74.50	78.12	76.53	76.59
	105.07	80.22	76.45	75.85	76.99	83.68	87.59	90.62
	110.30	93.11	81.91	88.15	86.88	87.75	92.75	94.94
$^2\Sigma^-$	29.89	8.51	−0.06	−10.00	−17.00	−22.68	−24.12	−23.50
	45.48[e]	26.10	27.88	31.24	35.59	44.30	48.28	48.84
	53.72	36.30	38.59	43.49	48.66	59.52	66.49	68.68
	74.67	56.75	50.87	65.20	71.74	65.89	67.48	70.50
	93.92	67.84	58.47	75.74	75.20	76.27	74.61	75.33
	102.56	82.82	75.76	83.50	76.65	79.79	78.54	78.52
$^2\Pi$	−41.41[f]	−55.00	−50.88	−38.85	−33.10	−25.58	−22.10	−21.10
	49.67	29.94	27.26	14.83	5.67	−0.89	−1.78	−1.33
	62.77	56.14	31.66	41.97	45.14	45.78	50.83	55.60
	92.27	58.35	51.88	46.73	47.67	56.97	63.86	65.99
	95.52	72.45	66.49	67.60	69.24	71.47	74.76	75.60
	100.74	73.55	75.04	72.93	74.79	75.72	75.42	78.03
$^2\Delta$	48.71	24.66	14.00	4.87	−1.18	−5.48	−6.04	−5.27
	53.94	35.76	37.01	43.15	48.81	58.10	64.67	66.48
	66.02	47.40	48.76	53.33	58.18	65.02	67.68	70.60
	74.62	60.92	65.27	65.45	71.37	72.67	74.31	75.09
	92.94	74.74	72.16	73.66	75.38	75.72	77.44	78.37
	94.29	76.08	75.90	82.44	78.94	84.17	89.58	90.35
$^4\Sigma^+$	104.29	78.81	72.76	75.22	75.96	77.14	75.50	74.32
	110.14	84.78	89.02	84.55	84.11	86.91	92.32	94.02
	113.09	115.83	116.30	109.55	110.93	100.89	96.59	95.31
	266.33	178.27	137.84	122.22	111.16	101.30	97.06	97.96
	271.58	180.29	139.25	123.30	111.69	111.25	110.03	109.69
	289.13	185.90	156.11	138.38	128.51	118.92	116.37	115.90
$^4\Sigma^-$	27.25	4.48	−6.18	−15.83	−21.20	−24.44	−24.47	−23.64
	44.70	25.22	25.68	30.00	33.83	35.35	37.00	39.95
	53.67	35.87	38.35	43.17	48.25	45.75	47.73	48.09
	92.00	62.25	48.70	62.80	50.65	58.75	59.12	59.88
	102.33	82.62	75.61	75.60	72.60	62.21	66.36	68.47
	108.44	89.14	84.30	82.06	76.46	72.51	71.93	73.35
$^4\Pi$	48.78	30.25	9.65	−2.15	−11.55	−19.17	−21.23	−20.88
	50.92	38.26	32.12	42.30	47.53	56.86	63.81	65.99
	95.05	44.79	52.89	59.89	64.32	68.00	66.24	66.96
	99.42	85.61	67.89	64.79	66.67	69.68	73.46	74.64
	109.71	87.83	84.58	77.84	76.44	72.30	76.64	77.14
	119.66	93.92	87.18	87.97	78.86	82.48	81.23	78.73
$^4\Delta$	53.89	35.69	36.95	43.13	48.80	58.45	65.08	66.89
	108.27	82.15	75.34	75.39	76.18	68.30	66.60	67.31
	114.01	89.12	89.98	85.46	77.08	77.44	75.75	74.52
	140.24	112.52	109.48	88.28	84.71	80.47	76.39	75.35
	255.88	154.99	122.02	102.55	90.58	87.16	90.88	92.41
	268.98	169.91	123.34	110.41	98.71	90.36	92.44	94.05

[a]Unit of energy = 1000 cm^{-1}.
[b]$A^2\Sigma^+$ state.
[c]$B^2\Sigma^+$ state.
[d]$C^2\Sigma^+$ state.
[e]$D^2\Sigma^-$ state.
[f]$X^2\Pi$ state.

TABLE 3. Energy differences between bottoms of potential energy wells of pairs of states (ΔT_e)[a]

States	Calculated ΔT_e[b]	Observed ΔT_e[c]
$X^2\Pi$–$A^2\Sigma^+$	34	32
$X^2\Pi$–$B^2\Sigma^+$	72	68
$X^2\Pi$–$C^2\Sigma^+$	97	88
$X^2\Pi$–$D^2\Sigma^-$	81	82
$A^2\Sigma^+$–$B^2\Sigma^+$	38	36
$A^2\Sigma^+$–$C^2\Sigma^+$	63	56
$A^2\Sigma^+$–$D^2\Sigma^-$	47	50
$B^2\Sigma^+$–$C^2\Sigma^+$	25	20
$B^2\Sigma^+$–$D^2\Sigma^-$	9	14
$C^2\Sigma^+$–$D^2\Sigma^-$	16	6

[a]Unit of energy = 1000 cm^{-1}.
[b]Calculated from Table 2.
[c]Calculated from data of Carlone and Dalby (1969) and Douglas[2].

about 17 000 cm^{-1}, which is to be compared with the experimental value of approximately 30 000 cm^{-1} (Carlone and Dalby 1969).

In Fig. 10 are shown our $A^2\Sigma^+$ curve, the $A^2\Sigma^+$ curve of Michels and Harris (1969), and an 'experimental' $A^2\Sigma^+$ curve. The latter was computed by the methods of Klein (1932) and Rydberg (1931, 1933) from the data in Table V of Carlone and Dalby (1969). The $A^2\Sigma^+$ curve of Michels and Harris (1969) is seen to be better than ours, which has a narrower well than the 'experimental' one. This narrowness is reflected in the fact that the $A^2\Sigma^+$ vibration frequency ω_e, as calculated from data in Table 2, is about 3865 cm^{-1}, which is about 25% higher than the observed value of 3180.56 cm^{-1} (Herzberg 1950).

A look at the $A^2\Sigma^+$ wave function reveals the presence of an appreciable $3p\pi$ component[3]. For reasons given earlier, the parameters for this orbital were optimized for a weighted average of the $^2\Sigma^+$ states, and it seems that this has adversely affected the lowest one. We would have obtained better energies for it had we been only interested in the lowest state.

Figure 9 shows that the $A^2\Sigma^+$ state is cut on the right side of the potential curve by three states which arise from $O(^3P)$ and $H(^2S)$, in the order $^4\Sigma^- < {}^2\Sigma^- < {}^4\Pi$ of increasing energy. This agrees with the calculations of Michels and Harris (1969). The predissociations in the $A^2\Sigma^+$ caused by these curve crossings are discussed by Czarny *et al.* (1971) and Gaydon and Kopp (1971).

Carlone and Dalby (1969) suggested that the C state may be highly ionic, and is probably H^+O^-. This suggestion is borne out by the present calculations. The dominant configuration of the $C^2\Sigma^+$ wave function is given in Table 1 to be $(1s)^2(2s)^2(2p\sigma)(2p\pi)^2(2p\tilde{\pi})^2$, which is composed of orbitals centered on oxygen.

In the same paper, Carlone and Dalby also suggested that the large spin doubling of the C state may be due to the levels of a similarly ionic $^2\Pi$ state close to the C state. The second excited $^2\Pi$ state is such a state. Its dominant configuration at 2.1 Å, the calculated equilibrium separation of the $C^2\Sigma^+$ state, is $(1s)^2(2s)^2(2p\sigma)^2(2p\pi)^2$-$(2p\tilde{\pi})$. Figure 9 shows that at that internuclear distance, the $^2\Pi$ curve is about 3000 cm^{-1} above the $C^2\Sigma^+$ curve. As noted in Part II*a*, the curves of Π symmetry are probably higher than non-Π curves at large internuclear separation by approximately 4000 cm^{-1}. A better calculation would then place the second excited $^2\Pi$ curve at or below the $C^2\Sigma^+$ curve at 2.1 Å. The $^2\Pi$ state possesses a number of highly excited vibrational levels whose vibrational wave functions are appreciable at that distance, and thus contribute strongly to the spin doubling.

The vibration frequency ω_e for $C^2\Sigma^+$, as calculated from data in Table 2, is about 1230 cm^{-1}, in very good agreement with the observed value 1232 cm^{-1} (Carlone and Dalby 1969).

(c) $^2\Sigma^-$ States

Figure 3 gives the $^2\Sigma^-$ curves. The lowest is predicted to be unbound. For the first excited $^2\Sigma^-$, the $D^2\Sigma^-$, the calculated equilibrium separation and the $X^2\Pi$–$D^2\Sigma^-$ energy difference agree very well with experiment (see Tables 1 and 3). Douglas[2] guessed that the $D^2\Sigma^-$ state consists of a $^3\Sigma^-$ core surrounded by a $(3s)_O$, or possibly a $(3p\sigma)_O$, Rydberg orbital. Table 1 shows that the main configuration at equilibrium consists of a $^3\Sigma^-$ core surrounded by a $3p\sigma$ molecular orbital. The next most important configuration, not listed in the table, has a $^3\Sigma^-$ core surrounded by a $3s$ molecular orbital[3]. The wave function is thus effectively a $^3\Sigma^-$ core plus an *s*–*p* hybrid molecular orbital.

The actual $D^2\Sigma^-$ curve is almost certainly shallower near its minimum than our curve. This is indicated by the fact that the zero-point vibrational frequency as calculated from Table 2, about 3673 cm^{-1}, is greater than the value deduced by Douglas[2] from the shift in the band origin between OH and OD, namely $\omega_e \simeq 2785$ cm^{-1}.

(d) Other States

No bound states of the OH radical of sym-

metry, other than $^2\Pi$, $^2\Sigma^+$, or $^2\Sigma^-$ have been observed experimentally. Figures 4 to 8 indicate that there are many bound states of $^2\Delta$, $^4\Sigma^-$, $^4\Sigma^+$, $^4\Pi$, and $^4\Delta$ symmetry which await discovery. There are also more bound states of $^2\Pi$, $^2\Sigma^+$, and $^2\Sigma^-$ symmetry.

No sextet spin states have been calculated here. However, there is a low-lying $^6\Sigma^-$ state which dissociates to $O(^5S)$ and $H(^2S)$ and which might be repulsive.

Concluding Remarks

One of the principal aims in undertaking these calculations was to obtain a broad qualitative insight into the electronic states of the OH radical which may be expected to exist within 100 000 cm^{-1} from the lowest state, as a help to experimental spectroscopists trying to disentangle the complicated emission spectrum of OH in the region 52 000 to 58 000 cm^{-1}, which contains over 1500 lines. It is very difficult to analyze this spectrum because individual rotational lines of a single band are widely separated, each band has several branches, different bands overlap, and several different electronic transitions occur in the same spectral region: It is therefore extremely difficult to associate any line with any particular band in the absence of some prior knowledge. It would therefore be of considerable help if one could predict, for instance, that a $^2\Pi$–$^2\Pi$ transition is to be expected in roughly this spectral region, and to estimate roughly what the rotational constants and spin-coupling types of the upper and lower states might be.

Indeed, tentatively this is what seems to be a possible interpretation of the more prominent groupings of lines in that spectrum, namely that they arise from the third $^2\Pi$ state, in transitions to high vibrational levels of the $X^2\Pi$ ground state. This example brings out the weaknesses as well as the strengths of our calculation. We predict a well-bound $^2\Pi$ state at around 85 000 cm^{-1}, with an estimated uncertainty $\pm 10\,000$ cm^{-1} (probably the error is less), whose equilibrium internuclear distance is about 1.2 Å (rotational constant B about 12 cm^{-1}). But a glance at Fig. 1 shows that two configurations are crossing and repelling one another around this distance. For any configuration interaction calculation in such a case, the calculated shape and position of the minimum are very sensitive to the quality of the molecular orbitals forming the two configurations. Nevertheless, even with this imprecision, the prediction is a very useful one.

Another aim was to get an idea of the possible effects of radiation on OH radicals in interstellar space. For instance, what are the likely photolytic transitions from the ground state, which will limit the life of OH? Or, is there a possibility that Lyman-α radiation falls close to an absorption line, thereby possibly giving rise to anomalous populations in the hyperfine structure sublevels of the ground state? A glance at Fig. 9 suggests, for instance, that Lyman-α radiation might cause weak transitions to the dissociating $^2\Delta$ state.

Within the limitations which we have discussed, the agreement of the present calculations with experiment on the known $^2\Pi$, $^2\Sigma^+$, and $^2\Sigma^-$ states, and with other calculations suggests that some trust may be placed in the other, as yet unverified, results from them.

Acknowledgments

The use of the facilities of the U.B.C. Computing Centre is gratefully acknowledged. The latter part of this work was carried out while one of the authors (I.E.) held a NRCC postgraduate scholarship.

CADE, P. E. and HUO, W. M. 1967. J. Chem. Phys. **47**, 614.
CARLONE, C. and DALBY, F. W. 1969. Can. J. Phys. **47**, 1945.
CAWTHON, T. M. and MCKINLEY, J. D. 1956. J. Chem. Phys. **25**, 585.
CHAMBERLAIN, J. W. and ROESLER, F. L. 1955. Astrophys. J. **121**, 541.
CZARNY, J., FELENBOK, P., and LEFEBVRE-BRION, H. 1971. J. Phys. B, **4**, 124.
DAS, G. and WAHL, A. C. 1967. J. Chem. Phys. **47**, 2934.
DIEKE, G. H. and CROSSWHITE, H. M. 1948. Bumblebee Series Report 87, The Johns Hopkins University, Baltimore, Maryland.
EASSON, I. 1971. M.Sc. Thesis, University of British Columbia, Vancouver, British Columbia.
FELENBOK, P. 1963. Ann. Astrophys. **26**, 393.
GAYDON, A. G. and KOPP, I. 1971. J. Phys. B, **4**, 752.
HERMAN, R. C. and HORNBECK, G. A. 1953. Astrophys. J. **118**, 214.
HERZBERG, G. 1950. Spectra of diatomic molecules (Van Nostrand Co., Inc., New York).
KLEIN, O. 1932. Z. Phys. **76**, 226.
MICHEL, A. 1957. Z. Naturforsch. **12a**, 887.
MICHELS, H. H. and HARRIS, F. E. 1969. Chem. Phys. Lett. **3**, 441.
MOORE, C. 1949. Atomic energy levels, NBS Circ. 467.
RYDBERG, R. 1931. Z. Phys. **73**, 376.
——— 1933. Z. Phys. **80**, 514.
TERZIAN, Y. and SCHARLEMANN, E. 1970. Earth Extraterr. Sci. **1**, 103.

This article has been cited by:

1. B Sourd, J Aubreton, M-F Elchinger, M Labrot, U Michon. 2006. High temperature transport coefficients in e/C/H/N/O mixtures. *Journal of Physics D: Applied Physics* **39**:6, 1105. [CrossRef]
2. B Grigorenko. 1998. Towards quantitative diatomics-in-molecules model for the water molecule. *Chemical Physics* **232**:3, 321-328. [CrossRef]
3. A Nemukhin. 1997. Ab initio potential functions for the ionic states of OH. *Chemical Physics Letters* **276**:3-4, 171-176. [CrossRef]
4. A VARANDAS, A VORONIN. 1995. Calculation of the asymptotic interaction and modelling of the potential energy curves of OH and OH. *Chemical Physics* **194**:1, 91-100. [CrossRef]
5. W Whitton. 1992. DIM potential energy surfaces for OH2+ (4A#). *Chemical Physics* **162**:2-3, 379-392. [CrossRef]
6. M Collard. 1991. Two-photon resonance ionisation spectroscopy of OH/OD D 2#-. *Chemical Physics Letters* **179**:5-6, 422-428. [CrossRef]
7. Y Bae. 1986. Observation of metastable autodetaching states of OH-. *Chemical Physics Letters* **126**:3-4, 266-272. [CrossRef]
8. V. Bermudez, M. Hoffbauer. 1984. Electron-stimulated desorption of neutrals from ionic surfaces: OH from TiO_{2}. *Physical Review B* **30**:2, 1125-1128. [CrossRef]
9. D Ramaker. 1983. Comparison of photon-stimulated dissociation of gas-phase, solid and chemisorbed water. *Chemical Physics* **80**:1-2, 183-202. [CrossRef]
10. S.V. Ljudkovski, A.V. Nemukhin, N.F. Stepanov. 1983. Diatomics-in-molecules studies of the Li + H2O interaction. *Journal of Molecular Structure: THEOCHEM* **104**:3-4, 403-409. [CrossRef]
11. R Day. 1983. Photoabsorption spectrum of radicals produced by a pulsed discharge of trace H2O in Ar. *Chemical Physics* **75**:1, 17-22. [CrossRef]
12. T Bergeman. 1980. Radiative properties of the B 2#+ and C 2#+ states in OH and OD. *Chemical Physics* **54**:1, 55-63. [CrossRef]
13. N Kouchi. 1979. Translational spectroscopy of electron-impact dissociative excitation of H2O and D2O by doppler profile measurements of Balmer-# emission. *Chemical Physics* **36**:2, 239-245. [CrossRef]
14. A. V. Nemukhin, N. F. Stepanov. 1979. Diatomics-in-molecules study of LiOH. *International Journal of Quantum Chemistry* **15**:1, 49-56. [CrossRef]
15. S Tsurubuchi. 1975. Correlation diagrams for electronic states of H2O and fragment species. *Chemical Physics* **10**:2-3, 335-344. [CrossRef]